COMPASS Force Field for 14 Inorganic Molecules, He, Ne, Ar, Kr, Xe, H_2, O_2, N_2, NO, CO, CO_2, NO_2, CS_2, and SO_2, in Liquid Phases

Jie Yang, Yi Ren, and An-min Tian

Chemistry Department, Sichuan Union University, Chengdu 610064, People's Republic of China

Huai Sun*,†

Molecular Simulations, Inc., San Diego, California 92121

Received: August 18, 1999; In Final Form: January 25, 2000

As a part of the COMPASS force field development, a number of small inorganic molecules were parametrized for condensed-phase applications. Using a simple valence model coupled with Coulomb energy and Lennard-Jones 9−6 functional terms, the parameters were optimized to yield accurate prediction of structural, vibrational, and thermophysical properties for these molecules. Extended validation on liquid nitrogen (N_2) and carbon dioxide (CO_2) in normal and supercritical conditions demonstrates that the present force field is capable of predicting various thermophysical properties in a very broad range of experimental conditions.

Introduction

Although most of the small inorganic molecules investigated in this work exist in gas phases under normal condition, they are frequently used in condensed phases, either as pure substances (fluids) or as additives or adsorbents in other bulk materials (polymers, zeolites, metal oxides, etc.). For example, supercritical CO_2 liquid has gained considerable attention in recent years. The continuing interest in diffusive properties of gas molecules in polymer matrixes is another good example. To conduct atomistic simulations of these small molecules in pure or mixed condensed phases, it is of great interest to prepare a generic and accurate force field.

We selected 14 common small molecules in this work. For convenience, these molecules are grouped into three categories—monatomic, He, Ne, Ar, Kr, and Xe; diatomic, H_2, O_2, N_2, CO, and NO; and triatomic, CO_2, NO_2, SO_2, and CS_2. Although various potential energy functions have been proposed for some of these molecules previously,[1,2] many of those potentials use special functional forms and almost all of them have been derived on the basis of a gas-phase data. Using special functional form makes it very difficult to apply the potentials to mixed systems since the force field parameters may be transferable only with the same functional forms. Due to lack of information about the electrostatic polarization and multibody interaction, parameters optimized using gas-phase data normally underestimate the intermolecular forces in condensed phases, leading to low densities and cohesive energies calculated for liquids or crystals.[3−6] In this work, we aimed to make a force field that is general and accurate for condensed-phase simulations. For the generality, we employed common functional forms that had already been used for many organic and inorganic functional groups in the COMPASS force field.[3] In addition, we ensured that the same parametrization principles that had been used previously were followed in this work. For accuracy, we utilized both gas-phase and liquid-phase properties to optimize the force field parameters. In particular, we used liquid data to optimize the nonbonded parameters, which led to a set of nonbonded parameters that accurately represent the effective interatomic interactions, especially in condensed phases.

Methodology

Due to the simplicity of the molecules in this work, a subset of the COMPASS functional forms[3] is used in this work. The total energy is written into valence contributions of bond stretching, angle deformation, cross-coupling of bond−bond and bond−angle, and nonbonded terms that include the electrostatic and van der Waals (vdW) terms.

$$\begin{aligned} E_{\text{total}} = & \sum_b [k_2(b-b_0)^2 + k_3(b-b_0)^3 + k_4(b-b_0)^4] && \text{bond} \\ & + \sum_\theta [k_2(\theta-\theta_0)^2 + k_3(\theta-\theta_0)^3 + k_4(\theta-\theta_0)^4] && \text{angle} \\ & + \sum_{b,b'} k_{b,b'}(b-b_0)(b'-b'_0) && \text{bond−bond} \\ & + \sum_{b,\theta} k_{b\theta}(\mathrm{b}-\mathrm{b}_0)(\theta-\theta_0) && \text{bond−angle} \\ & + \sum_{i,j} \frac{q_i q_j}{r_{ij}} && \text{coulombic} \\ & + \sum_{i,j} \epsilon_{ij}\left[2\left(\frac{r^o_{ij}}{r_{ij}}\right)^9 - 3\left(\frac{r^o_{ij}}{r_{ij}}\right)^6\right] && \text{vdW} \end{aligned} \quad (1)$$

The subscripts *i* and *j* represent pairs of atoms that are separated by two or more intervening atoms, or those that belong to different molecules. The Lennard-Jones 9−6 (LJ-9−6) function is a crucial component for predicting condensed-phase properties. On the basis of numerous validation studies,[3−6] this function is capable of representing the effective van der Waals interactions in the common atom−atom separation region so that many physical properties of molecular liquids and crystals can be well reproduced.

† Current address: Agouron Pharmaceuticals, Inc., 3550 General Atomics Court, San Diego, CA 92121.

10.1021/jp992913p CCC: $19.00
Published on Web 04/27/2000

The LJ-9−6 parameters (ϵ_0 and r_o) are given for homatomic pairs. For heteratomic pairs, a sixth-order combination law[7] is used to calculate the corresponding parameters:

$$r_{ij}^{o} = \left(\frac{(r_i^o)^6 + (r_j^o)^6}{2}\right)^{1/6} \tag{2}$$

$$\epsilon_{i,j} = 2(\epsilon_i \epsilon_j)^{1/2} \frac{(r_i^o)^3 (r_j^o)^3}{(r_i^o)^6 + (r_j^o)^6} \tag{3}$$

The coulombic interaction term is used for molecules that contain polarized chemical bonds so that distributed partial charges are used to represent the electrostatic potential energy surfaces. In the COMPASS force field, the partial charges are calculated from the charge bond increment, δ_{ij}, which represents charge separation between two valence-bonded atoms.[3] The net charge q_i for atom i is a summation of all charge bond increments related to atom i:

$$q_i = \sum_j \delta_{ij} \tag{4}$$

The charge parameters are usually determined by fitting to the ab initio electrostatic potentials (ESP) of molecules. To maintain the transferability, a constrained ESP (CESP) method[3] was used in which any previously determined bond increments were transferred and fixed while only the unknown parameters were relaxed to fit the electrostatic potentials.

For diatomic molecules, only a bond stretching function is used as the valence term. Although the valence parameters can be generally determined from ab initio data in COMPASS development, an empirical method is more efficient for simple diatomic molecules because of the availability of high-quality experimental data. The useful data are equilibrium bond length r_0, dissociation energy D_e, and harmonic frequency $\tilde{\nu}$ or force constant k_e. With these data, the force constants of the bond term can be easily derived on the basis of Taylor expansion of the Morse function:

$$\begin{aligned} k_2 &= D_e a^2 = (1/2)k_e \\ k_3 &= -D_e a^3 = -k_2 a \\ k_4 &= (7/12)D_e a^4 = -(7/12)k_3 a \end{aligned} \tag{5}$$

where $a = (k_e/2D_e)^{1/2}$.

For triatomic molecules, the normal COMPASS development procedure was followed to derive the valence parameters. First, the charge parameters were determined using the CESP method. With the charge parameters and a set of approximated vdW parameters fixed, the valence parameters, including all cross-coupling terms, were derived by fitting to the ab initio energies and the first and second derivatives of the energies. The parameters were then scaled or modified to fit available experimental data.

For all molecules studied in this work, the vdW parameters were optimized based on molecular dynamics simulations of liquids. Two types of observables, equilibrium densities and cohesive energies, were used to determine the parameters. Constant-volume (NVT) simulations were carried out during the parametrization stage since it is less computationally complex (only one variable needs to be controlled) than the constant-pressure (NPT) method. Therefore, average pressures at given temperatures and densities were evaluated and compared with the experimental pressure (mostly at 1 atm). For liquids, the cohesive energy (E_{coh}) is related to the experimentally measured heat of vaporization H_v:

$$E_{coh} = H_v - RT \tag{6}$$

An assumption that the vapor phase obeys the ideal gas law is underlying formula 6. The heat of vaporization can be obtained from the literature or calculated from the temperature dependence of vapor pressure using the Clausius−Clapeyron equation:

$$H_v = R \frac{d \ln P}{d(1/T)} \tag{7}$$

The simulation conditions were carefully examined, and the following parameters were found adequate for obtaining consistent and reliable results. The unit cells normally contained about 1000 atoms, with the cell dimensions in the range of 20−25 Å. The nonbonded interactions, both vdW and electrostatic terms, were evaluated using charge-group-based cutoff. The tail corrections were added for the vdW interactions. Using neutral groups as the nonbonded cutoff units avoids expensive Ewald summation without losing accuracy in the calculation[3] of electrostatic energies. The cutoff values were usually between 8.5 and 10.0 Å. The velocity Verlet method, with a 1 fs time step, was used as the integrator in all simulations. The random velocity scaling method[8] was used to control the temperature. In the NVT simulation, the pressure and cohesive energy were evaluated by averaging over 50 ps of trajectory, which was taken after the 50−100 ps preequilibration. After the parametrization, NPT simulations with a pressure-bath coupling method proposed by Berendsen[9] were carried out for validation purposes. From the NPT simulations, the average densities were calculated by averaging over 100 ps trajectory.

Ab initio software packages Turbomole[10,11] were used to calculate the energies, energy derivatives and atomic partial charges. The valence and cross-coupling parameters were derived using a general least-squares-fitting program, PROBE.[11] All molecular mechanics and molecular dynamics simulations were carried out using DISCOVER.[11]

TABLE 1: Experimental Data and NVT Simulation Results for Monatomic Liquids

	exptl[10,11]			calcd	
molecule	T (K)	D (g/cm^3)	H_v (kcal/mol)	P (bar)	H_v (kcal/mol)
helium	4.2	0.125	0.02	3 ± 0	0.02 ± 0.01
neon	27.1	1.205	0.41	26 ± 1	0.41 ± 0.01
argon	87.3	1.393	1.54	-3 ± 4	1.54 ± 0.01
krypton	119.8	2.414	2.17	3 ± 6	2.17 ± 0.01
xenon	161.4	2.984	3.02	2 ± 5	3.02 ± 0.01

Results and Discussions

Monatomic Molecules. The experimental data used for parametrizing the inert gas molecules are summarized in Table 1. We found significant discrepancies in the equilibrium densities of liquid krypton and xenon in the literature. The values given in the CRC handbook[12] are 2.155 g/cm^3 at 119.78 K for krypton and 3.520 g/cm^3 at 173 K for xenon; both are given without references so that the detailed information on the experimental condition is unknown. However, 2.4138 g/cm^3 at 119.78 K and 1 atm for saturated liquid krypton and 2.9844 g/cm^3 at 161.36 K and 1 atm for saturated liquid xenon are given by Rabinovich et al.[13] The latter data, which appear to be consistent with the extensive data of the equation of state reported by the same authors and others,[13] were used in this work.

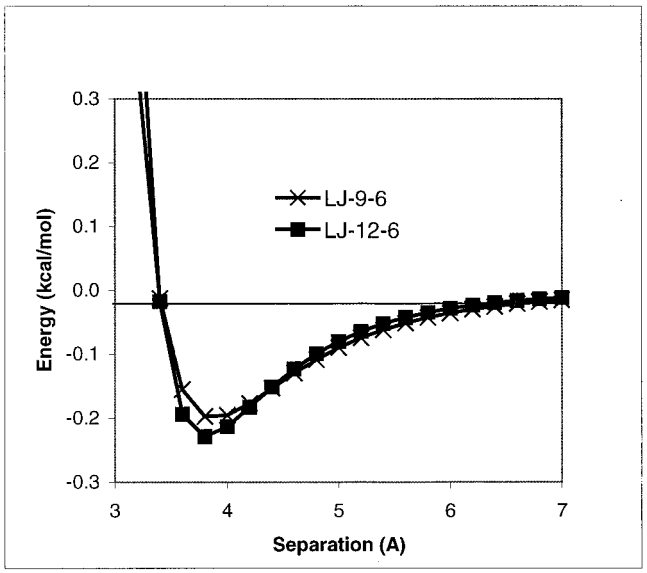

Figure 1. Comparison of LJ-12−6 and LJ-9−6 functions optimized for liquid argon.

The NVT simulation results with the optimized parameters are also listed in Table 1. Since the number of parameters (two, r_0 and ϵ) are equal to the number of observables, the final results basically reproduce those used for the parametrization with statistical errors. The calculated pressures are very close to the experimental pressures (1 bar); the values of the heat of vaporization obtained are identical to the experimental values. The standard deviations given in this and several other tables in this paper are estimated true variances[3] of statistically independent measurements from the simulation, which were estimated using the following formula:

$$\sigma = (\tau_A/\tau_{run})^{1/2}\sigma_{run} \tag{8}$$

where τ_{run} is the total run time (50 000 fs for NVT and 100 000 fs for NPT in this work), σ_{run} is the variance obtained in the calculation, and τ_A is the estimated correlation time. On the basis of a study reported in a previous publication,[3] a reasonable value of τ_A is 250 fs for the pressure, 500 fs for the energy, and 3000 fs for the density.

The optimized vdW parameters, r_0 and ϵ, together with definitions of atom types and all other parameters, are given in the Appendix. Because of the difference in the functional forms, it is not meaningful to directly compare the vdW parameters with those published in the literature. However, it is of interest to compare the different functions parametrized in the same manner. For this reason, we parametrized both LJ-9−6 and LJ-12−6 functions for argon liquid. The results are plotted in Figure 1. In comparison with the LJ-12−6 function, the 9−6 function is "softer" at the repulsive region ($E > 0$) and more attractive at large separation ($r \gg r_0$). Since the parameters are optimized on the basis of configurations in which the atoms are separated from short distance (repulsive region) to infinite distance, the LJ-9−6 well depth is shallower and the vdW radius is larger than those of the 12−6 function.

Using the optimized parameters, we carried out NPT simulations along the experimental solidification curves[13] to validate the force field. The calculated densities at different temperatures and pressures are compared with the experimental values in Table 2. The percentage errors are summarized in the last column of this table. Generally speaking, the densities obtained agree very well with the experimental values for all but liquid helium. The relatively large deviation found in the helium is presumably due to their small absolute values (<0.26 g/cm^3). In addition, this may indicate the difficulty of modeling extremely light molecules at very low temperatures using classical methods.

TABLE 2: Comparison of Experimental[11] and NPT-Simulated Densities of Monatomic Liquids

			D (g/cm^3)		
molecule	T (K)	P (bar)	exptl	calcd	err (%)
helium	4.2	1.0	0.125	0.121	−3.2
	4.2	7	0.145	0.132	−9.0
	3.0	1.0	0.143	0.129	−10.2
	3.0	80.0	0.203	0.234	15.2
	98.2	1000	0.209	0.253	21.0
neon	27.1	1.0	1.205	1.199	−0.5
	25.0	30.5	1.254	1.263	0.7
	32.0	540.5	1.341	1.371	2.2
	38.0	1039.0	1.400	1.446	3.3
argon	87.3	1.0	1.393	1.399	0.4
	94.7	451.0	1.463	1.479	1.1
	100.8	721.0	1.486	1.518	2.2
	108.1	1051.0	1.506	1.539	2.2
krypton	119.8	1.0	2.414	2.425	0.5
	115.8	0.7	2.458	2.461	0.1
	130.0	491.7	2.519	2.564	1.8
	145.0	1044.0	2.580	2.632	2.0
xenon	161.4	0.8	2.984	2.980	−0.1
	165.0	1.0	2.941	2.961	0.7
	180.0	493.7	3.077	3.085	0.2
	200.0	1058.0	3.164	3.188	0.8

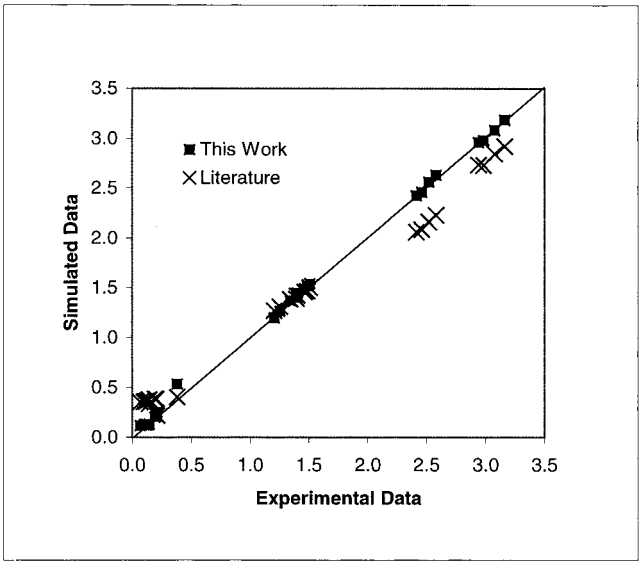

Figure 2. Comparison of calculated and experimental densities of nobel gas molecules. Two sets of calculated data are obtained using this and literature potentials.

In Figure 2, we plotted a correlation chart of the calculated and experimental densities[11,13] of inert gas molecules in liquid states. For comparison, we used both the new COMPASS potentials presented in this work and LJ-12−6 potentials reported in the literature[1,2] in the simulation. Our results agree very well with the experimental values; however, the results using literature potentials that are mostly derived from gas-phase properties show large deviations. This chart demonstrates that, even for inert gas molecules, which have very weak intermolecular interactions in general, it is necessary to parametrize the force field explicitly for condensed-phase applications. This is especially true for simple Lennard-Jones functional forms.

Diatomic Molecules. The empirical data[12,14] used for parametrizing the diatomic molecules are listed in Table 3. The

TABLE 3: Empirical Data for Deriving Valence Parameters of Diatomic Molecules

molecule	b_0 (A)	ν (cm^{-1})	D_e (kcal/mol)	μ (D)
H_2	0.7412	4403.2	109.49	0
N_2	1.0977	2358	271.96	0
O_2	1.2074	1580.2	120.21	0
NO	30.01	1904	186.4329	0.159
CO	1.1283	2169.8	258.8686	0.11

TABLE 4: Experimental Data and NVT Simulation Results for Diatomic Liquids

	extpl			calcd	
molecule	T (K)	D (g/cm^3)	H_v (kcal/mol)	P (bar)	H_v (kcal/mol)
H_2	20.4	0.071	0.22	5 ± 9	0.22 ± 0.01
N_2	77.3	0.807	1.32	-1 ± 45	1.34 ± 0.01
O_2	90.2	1.136	1.62	22 ± 51	1.62 ± 0.01
NO	123.0	1.269	3.31	-4 ± 67	3.16 ± 0.01
CO	81.7	0.789	1.44	28 ± 49	1.44 ± 0.01

equilibrium bond lengths (b_0), normal model frequencies (ν), and bond dissociation energies (D_e) were used to derive the valence parameters. The experimental dipole moments (μ), together with the equilibrium bond lengths, were used to determine the atomic partial charges for nitric oxide (NO) and carbon monoxide (CO).

In Table 4, the equilibrium density (D) and heat of vaporization (H_v) at the boiling point (T_b) for each of the molecular liquids[15] are listed. These data were used for parametrizing the vdW parameters. It was straightforward to derive the vdW parameters for hydrogen, oxygen, and nitrogen molecules in the same manner as that for the monatomic molecules. However, for nitric oxide or carbon monoxide, four parameters for two atom types need to be parametrized. Using the limited data set, we reduced the adjustable parameters to two scaling factors (k_ϵ and k_r for ϵ_0 and r_0, respectively) that multiply a set of estimated vdW parameters (ϵ_0 and r_0) to make the final parameters for each of the atom types:

$$\begin{aligned} \epsilon_0(\mathrm{M1}) &= k_\epsilon \epsilon_0^*(\mathrm{M1}) \\ \epsilon_0(\mathrm{M2}) &= k_\epsilon \epsilon_0^*(\mathrm{M2}) \\ r_0(\mathrm{M1}) &= k_r r_0^*(\mathrm{M1}) \\ r_0(\mathrm{M2}) &= k_r r_0^*(\mathrm{M2}) \end{aligned} \tag{8}$$

where M1 and M2 denote different atom types. The estimated vdW parameters (ϵ_0^*, r_0^*) were calculated using the ESFF force field[9] on the basis of atomic properties (ionization potentials, etc.), London's formula, and the harmonic oscillator model of atomic polarizability.

The final parameters, including both valence (bond) and nonbonded parameters, are listed in the Appendix. With these parameters, the same structural and vibrational properties as given in Table 3 can be reproduced. The NVT simulation results of liquid properties are given in Table 4. The calculated average pressures are within ±30 bar from the target pressure (1 atm), and the values of heat of vaporization (H_v) are a few percents different from the experimental data. The standard deviations for the calculated values of pressure and heat of vaporization were calculated using eq 8. The small deviations between the calculated and experimental pressures correspond to minimal errors in the densities of NPT simulations. As given in Table 5, the averaged densities calculated agree very well (about 1% relative percentage error) with the experimental values.

TABLE 5: Comparison of Experimental and NPT-Simulated Densities of Diatomic Liquids

			D (g/cm^3)		
molecule	T (K)	P (bar)	exptl	calcd	err (%)
H_2	20.4	1.000	0.071	0.071	0.0
N_2	77.3	1.000	0.807	0.804	−0.4
O_2	90.2	1.000	1.136	1.122	−1.2
CO	81.7	1.000	0.789	0.786	−0.4
NO	123.0	1.000	1.269	1.269	0.0

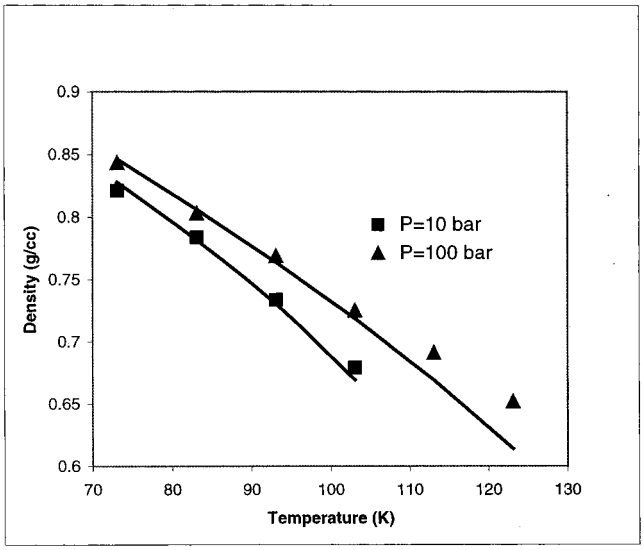

Figure 3. Comparison of Calculated (dots) and experimental (lines) isobaric equation of states of liquid nitrogen.

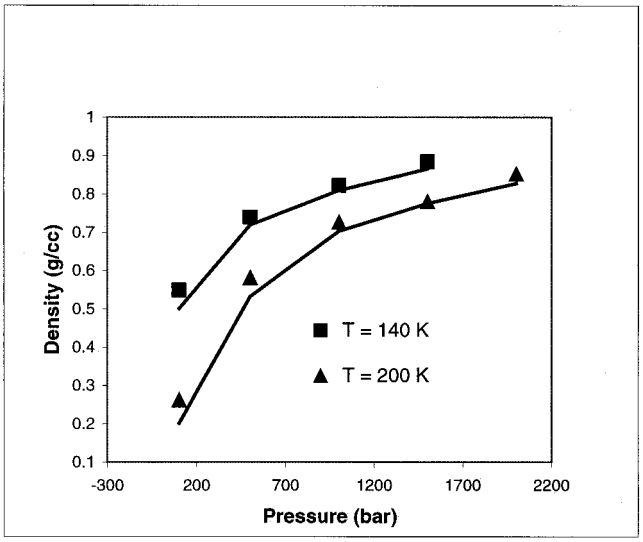

Figure 4. Comparison of calculated (dots) and experimental (lines) isothermal equation of states of super critical liquid nitrogen.

Liquid nitrogen is one of the most common solvents used in laboratories. Taking it as an example, we carried out extensive NPT simulations with the optimized parameters to test whether the parameters can be extrapolated to predict the thermophysical properties outside the parametrization domain. Two experimental isobaric lines[16] (P = 10 and 100 bar) of liquid nitrogen from 70 to 120 K are plotted in Figure 3, with the calculated values (dots in the figure) for comparison. Under 100 K, the agreement is excellent; the percentage errors between the calculated and experimental data are with in 1%. Above 100 K, the system is close to the critical point (T_c = 126 K), and slightly larger errors are obtained. For example, at P = 100 bar, the densities

TABLE 6: Comparison of Experimental and Calculated Intramolecular Properties of Triatomic Molecules

molecule	property	exptl	calcd
CO_2	B_0 (Å)	1.160	1.163
	θ (deg)	180.0	180.0
	μ (D)	0.0	0.0
	ν_1 (cm^{-1})	2349	2351
	ν_2 (cm^{-1})	1333	1384
	ν_3 (cm^{-1})	667	659
CS_2	B_0 (Å)	1.553	1.554
	θ (deg)	180.0	180.0
	μ (D)	0.0	0.0
	ν_1 (cm^{-1})	1535	1539
	ν_2 (cm^{-1})	658	669
	ν_3 (cm^{-1})	397	402
NO_2	B_0 (Å)	1.193	1.193
	θ (deg)	134.1	134.1
	μ (D)	0.316	0.326
	ν_1 (cm^{-1})	1618	1625
	ν_2 (cm^{-1})	1318	1312
	ν_3 (cm^{-1})	750	737
SO_2	B_0 (Å)	1.431	1.431
	θ (deg)	119.3	119.3
	μ (D)	1.633	1.634
	ν_1 (cm^{-1})	1362	1361
	ν_2 (cm^{-1})	1151	1164
	ν_3 (cm^{-1})	518	514

TABLE 7: Experimental Data and NVT Simulation Results for Triatomic Liquids

	extpl			calcd	
molecule	T (K)	D (g/cm^3)	H_v (kcal/mol)	P (bar)	H_v (kcal/mol)
CO_2	216.6	1.179	3.65	-32 ± 103	3.67 ± 0.01
NO_2	293.2	1.446	9.11	-44 ± 108	8.99 ± 0.01
SO_2	223.2	1.557	6.51	-120 ± 84	6.47 ± 0.01
CS_2	293.2	1.262	6.62	-28 ± 72	6.57 ± 0.01

TABLE 8: Comparison of Experimental and NPT-Simulated Densities of Triatomic Liquids

			D (g/cm^3)		
molecule	T (K)	P (bar)	exptl	calcd	err (%)
CO_2	216.6	1.0	1.179	1.167	−1.0
NO_2	293.2	1.0	1.446	1.446	0.0
SO_2	223.2	1.0	1.557	1.577	1.3
CS_2	293.2	1.0	1.262	1.273	0.9

calculated at 113 and 123 K are 3.3% and 6.2%, respectively, higher than the corresponding experimental values.

In Figure 4, the calculated densities are compared with the experimental data[16] for supercritical liquid nitrogen. The data are plotted along two isotherm lines, $T = 140$ and 200 K, while the pressure varies from 100 to 2000 bar. As shown in the figure, excellent agreement is obtained. Only at the low-density region, the differences between the calculated and measured data are slightly sizable.

It should be emphasized that the parameters were optimized using two observables (density and cohesive energy) measured at one $P-T$ (pressure and temperature) point, as given in Table 3. The results plotted in Figures 3 and 4 demonstrate that the single-point optimized parameters can be used to predict accurately the thermophysical properties of liquid nitrogen in a very broad range of experimental conditions, below and above the critical point, without modifying the parameters or introducing new parameters. This observation demonstrates the validity of using the LJ-9−6 function to represent effective vdW energies for organic molecules in liquid states. We also found that similar results can be obtained by using LJ-12−6 function.

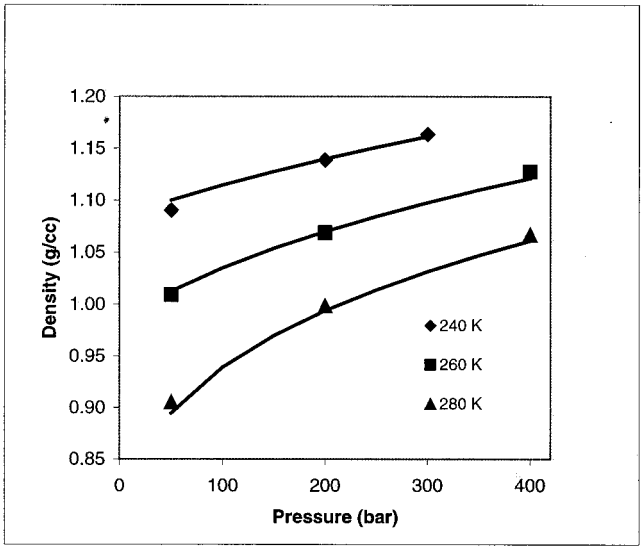

Figure 5. Comparison of calculated (dots) and experimental (lines) isothermal equations of state of liquid carbon dioxide.

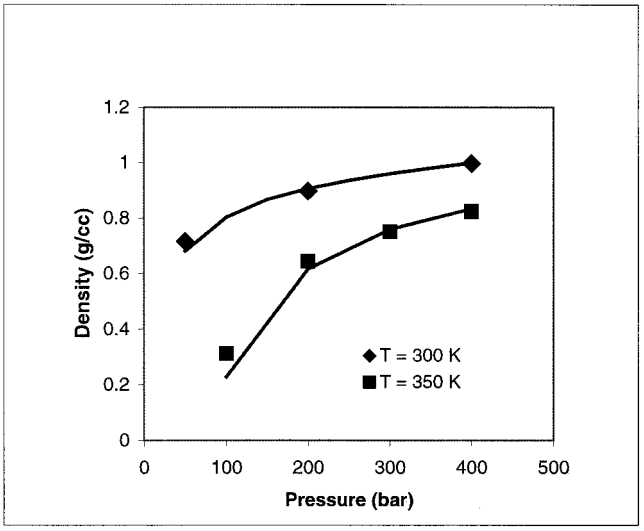

Figure 6. Comparison of calculated (dots) and experimental (lines) isothermal equation of states of super critical liquid carbon dioxide.

Triatomic Molecule. Valence and charge parameters for triatomic molecules were derived from the ab initio data. First, the atomic partial charges were determined by fitting to the electrostatic potentials, calculated at the HF/6-31G* level with the optimized structure for each of the molecules. The values were converted into bond increments as given in the Appendix. Then, with the partial charges and a set of initial vdW parameters fixed, we derived the valence parameters by fitting to ab initio energies, first and second derivatives of energies, calculated for each of the molecules. To determine the nonharmonic and cross-coupling parameters, distorted structures were included in the ab initio calculations. The resulted parameters were subsequently adjusted to yield better agreement with the experimental data of structures and frequencies.

After the valence and charge parameters were determined, the trial vdW parameters were optimized using MD simulation of liquids. In each of these simulations, the number of adjustable parameters was limited to two by transferring parameters.[3] Specifically, parameters of the carbon atom in carbon dioxide and carbon disulfide were taken from non aromatic sp^2 (alkene) carbon (atom type C2 = $r_0 = 3.915$, $\epsilon_0 = 0.068$), and the parameters of the oxygen atom in sulfur dioxide and nitric

dioxide were taken from the oxygen of the carbonyl group (atom type o1=, $r_0 = 3.43$, $\epsilon_0 = 0.192$).

Finally, the valence parameters were subjected to minor adjustments to ensure that overall good fits to the experimental observables[12] are maintained after the modification of vdW parameters. The final parameters are given in the Appendix. In Table 6, comparisons of molecular structures, dipole moments, and vibrational frequencies between the force field calculation and the experimental measurement are given.

Table 7 lists the NVT simulation results with the optimized parameters. Similar to those obtained for monatomic and diatomic molecules, both average pressures and cohesive energies are in good agreement with the experimental values. Again, the standard deviations were calculated using eq 8. The average densities, obtained using NPT simulation, are given in Table 8. Consistent with the NVT results, the calculated densities are in excellent agreement with the experimental data. The percentage errors are approximately less than 1%.

Extensive NPT simulations were carried out for liquid CO_2. Experimental isothermal lines[17] are plotted in Figures 5 and 6, with the calculated data (dots) for comparison. In Figure 5, the data for CO_2 liquid under normal conditions are plotted. For T = 240, 260, and 280 K, the isothermal lines are reproduced very well in a broad range of pressures ranging from 50 to 400 bar. The isothermal lines above the critical point are plotted in Figure 6. At 300 K, the agreement between calculated and measured is excellent. At 350 K, however, a relatively larger deviation is observed at the low-density region, which is similar to that obtained for liquid nitrogen.

Conclusions

In this paper, we present a set of molecular force field parameters for 14 common small inorganic molecules, with emphasis on their liquid-phase applications. For monatomic and diatomic molecules, the parameters were derived empirically. For triatomic molecules, the valence and electrostatic parameters were first derived using ab initio data and then optimized to fit the empirical data; the vdW terms were parametrized empirically. Equilibrium density and cohesive energy at a single point of temperature and pressure were used to derive the vdW parameters for each of the molecules.

The force field parameters were validated against the training data set. In addition, extended calculations were performed to calculate data points outside the training set, which provides much more rigorous tests not only on the parameters but also on the functional forms. Using two examples, fluid nitrogen and carbon dioxide, we demonstrated that the parameters obtained are good for predicting the equations of state for these molecules in a very broad range of experimental conditions. For normal and supercritical liquid states, the predicted equilibrium densities agree well with the experimental data. The curvatures of $P-V-T$ lines, representing the thermal expansion coefficients or compressibility coefficients, are in excellent agreement with the experimental observations.

Because the same parametrization method and procedure were taken in developing all parameters presented in this paper, we expect very similar results for all other molecular liquids covered in this paper can be obtained. In addition, since consistent functional forms and parametrization principles were used in the development of all COMPASS parameters, the present force field parameters should work well together with other COMPASS parameters in dealing with mixed systems. Further validation and application are underway.

Acknowledgment. This work was partially supported by the National Natural Science Foundation of China (Project Number 29603005). J.Y. thanks MSI for a kind invitation of visiting during the preparation of this manuscript.

Appendix. Parameters for 14 Small Inorganic Molecules[a]

Atom Types

he	helium	o1c	oxygen in CO
ne	neon	n1o	nitrogen in NO
ar	argon	o1n	oxygen in NO
kr	krypton	c2=	carbon in CO_2 and CS_2
xe	xenon	n2o	nitrogen in NO_2
h1h	hydrogen in H2	o1=*	oxygen in CO_2
n1n	nitrogen in N_2	o1=	oxygen in NO_2 and SO_2
o1o	oxygen in O_2	s2=	sulfur in SO_2
c1o	carbon in CO	s1=	sulfur in CS_2

Bond Increment

i	j	δ_{ij}	i	j	δ_{ij}
c1o	o1c	−0.0203	n1n	n1n	0.0000
c2=	o1=	0.4000	n1o	o1n	0.0288
c2=	s1=	0.0258	o1=	s2=	−0.2351
n2o	o1=	0.0730	o1o	o1o	0.0000
h1h	h1h	0.0000			

Bond

i	j	b_0	k_2	k_3	k_4
h1h	h1h	0.7412	414.2185	−805.6549	914.1296
n1n	n1n	1.0977	1651.3730	−4069.3178	5984.9629
o1o	o1o	1.2074	846.7150	−2247.1760	3478.9900
c1o	o1c	1.1283	1368.7676	−3157.0007	4247.5298
n1o	o1n	1.1506	1147.8362	−3167.7349	5099.5811
o1=	s2=	1.4308	730.8387	−1531.7910	1859.7753
c2=	o1=	1.1600	1161.3421	−2564.5706	3932.8735
n2o	o1=	1.1930	620.0000	−1808.6018	3077.5918
c2=	s1=	1.5540	559.0065	−1348.6633	1248.8604

Angle

i	j	k	θ_0	k_2	k_3	k_4
o1=	c2=	o1=	180.0000	57.1000	0.0000	0.0000
s1=	c2=	s1=	180.0000	48.0000	0.0000	0.0000
o1=	n2o	o1=	134.1000	150.0000	−82.1013	−40.0005
o1=	s2=	o1=	119.3000	115.2627	−35.6278	−26.1261

Bond−Bond

i	j	i'	$k_{bb'}$
o1=	c2=	o1=	275.4350
s1=	c2=	s1=	100.7369
o1=	n2o	o1=	20.0000
o1=	s2=	o1=	20.0000

Bond−Angle

i	j	i'	$k_{b\theta}$
o1=	n2o	o1=	−50.0000
o1=	s2=	o1=	45.0585

LJ-9−6

i	r_0	ϵ_0	i	r_0	ϵ_0
he	2.9000	0.00500	o1c	3.6020	0.08500
ne	3.2000	0.05500	n1o	3.4600	0.12800
ar	3.8800	0.20000	o1n	3.3000	0.15600
kr	4.3000	0.28000	c2=	3.9150	0.06800
xe	4.2600	0.39000	s2=	4.0470	0.12500
h1h	1.4210	0.02160	n2o	3.5290	0.33300
n1n	3.8008	0.05980	o1=	3.4300	0.19200
c1o	4.0120	0.05300	o1=*	3.3600	0.06700
o1o	3.4758	0.07800	s1=	4.0070	0.31300

[a] Units: lengths, Å, angle, degree, energy, kcal/mol.

References and Notes

(1) Martland, G. C.; Rigby, M.; Smith, E. B.; Wakeham, W. A. *Intermolecular Forecs: Their Origin and Determination;* Clarendon Press: Oxford, 1981.

(2) Hirschfelder, J. O.; Curtiss, C. F.; Bird, R. B. *Molecular Theory of Gases and Liquids*; Wiley: New York, 1954.

(3) Sun, H. *J. Phys. Chem.* **1998**, *B102*, 7338.

(4) Sun, H.; Rigby, D. *Spectrochimica Acta A* **1997**, *53*, 1301.

(5) Rigby, D.; Sun, H.; Eichinger, B. E. *Polym. Int.* **1997**, *44*, 311.

(6) Sun, H.; Fried, J. R.; Ren, P., *Theoretical Comput. Theor. Polym. Sci.* **1998**, *8*, 229.

(7) Waldman, M.; Hagler, A. T. *J. Comput. Chem.* **1993**, *14*, 1077.

(8) Andrea, T. A.; Swope, W. C.; Andersen, H. C. *J. Chem. Phys.* **1983**, *79*, 4576.

(9) Berendsen, H. J. C.; Postma, J. P. M.; van Gunsteren, W. F.; DiNola, A.; Haak, J. R. *J. Chem. Phys.* **1984**, *81*, 3684.

(10) Ahlrichs, R.; Baer, M.; Haeser, M.; Horn, H.; Koehmel. *Chem. Phys. Lett.* **1989**, *162*, 165.

(11) Turbomole, PROBE, DISCOVER, and ESFF are software packages distributed by Molecular Simulations Inc., San Diego, CA.

(12) *Handbook of Chemistry and Physics*; Lide, D. R., Ed.; CRC Press: Boca Raton, FL, 1995.

(13) Rabinovich, A. V.; Vasserman, A. A.; Nedostup, V. I.; Veksler, L. S. In *Thermophysical Properties of Neon, Argon, Krypton and Xenon*; Selover, T. B., Jr., Ed.; Hemisphere Press: Bristol, PA, 1988.

(14) Huber, K. P.; Herzberg, G. *Molecular Spectra and Molecular Structure IV. Constants of Diatomic Molecules*; Van Nostrand Reinhold Co.: New York, 1979.

(15) Beaton, C. F.; Hewitt, G. F. *Physical Property Data for the Design Engineer*; Hemisphere Press: Bristol, PA, 1989.

(16) Jacobsen, R. T.; Stewart, R. B.; Jahangiri, M. *J. Phys. Chem. Ref. Data*, **1986**, *15* (2), 735−909. Electronic formatted data are available in the *NIST Chemistry WebBook*, http://webbook.nist.gov/chemistry/.

(17) Ely, J. F.; Magee, J. W.; Haynes, W. M. Research Report RR-110; Gas Processors Association: Tulsa, OK, 1987. Electronic formatted data are available in the *NIST Chemistry WebBook*, http://webbook.nist.gov/chemistry.